Low-loss infrared dielectric material system for broadband dual-range omnidirectional reflectivity

B. Temelkuran, E. L. Thomas, J. D. Joannopoulos, and Y. Fink

Massachusetts Institute of Technology, 77 Massachusetts Avenue, Cambridge, Massachusetts 02139

A material system for broadband thermal IR applications based on branched polyethylene and tellurium is introduced. This system exhibits low absorption losses from 3.5 to 35 μm, has a large index contrast, and is readily deposited as a thin film. These unique features were used to investigate the formation of an omnidirectional reflector that exhibits two distinct, broadband omnidirectional ranges at thermal wavelengths. Reflectivity measurements are presented that confirm the existence of two omnidirectional ranges in the solar atmospheric windows extending from 8 to 12 μm and from 4.5 to 5.5 μm. The measurements are in good agreement with simulations.   © 2001 Optical Society of America

OCIS codes: 160.5470, 310.0310, 230.1480, 230.3060.

Photonic crystals are periodic structures that inhibit the propagation of electromagnetic waves of certain frequencies and provide a mechanism for controlling the flow of light.[1,2] Considerable effort has been devoted to the construction of three-dimensional periodic structures at length scales ranging from the microwave to the visible.[3–5] However, the technological difficulties and the cost of fabrication severely limit the utilization of these three-dimensional structures for thermal and optical frequency applications. Two-dimensional periodic structures that can confine the light in the plane of periodicity only and that are easier to fabricate have also been investigated.[6] Recently, it was shown both experimentally and theoretically that under certain conditions a one-dimensional periodic structure could be used to reflect electromagnetic waves that were incident from all directions and any polarization.[7–9] This structure, which is simple to fabricate, leads naturally to many application opportunities, including telecommunications, optoelectronics, and thermal radiation.[8,9] Nevertheless, a critical issue involves the choice of the materials and their processing. In this Letter we present a new low-loss material combination and demonstrate an omnidirectional reflector that exhibits two distinct omnidirectional ranges at thermal wavelengths.

Many of the useful properties of photonic crystals depend on gap size, which increases with increasing index contrast. To achieve high reflectivity values, one needs an evanescent decay length that is much smaller than the absorption length; hence, material systems with a large index contrast and low absorption are preferred.

With its high refractive index and very low absorption, Te is a suitable choice of material for these structures. Previously, a Te and polystyrene material system was used to fabricate an omnidirectional photonic crystal at thermal wavelengths. However, because it has a large number of vibrational absorption modes,[10] polystyrene is not the best choice for achieving high reflectivities across a wide range of the IR portion of the spectrum.

Identifying a low-index, low-loss material at thermal wavelengths that can be easily processed and that

has good mechanical and environmental stability is challenging. Typical inorganic low-index materials either have absorption problems at these thermal wavelengths (such as oxides) or are simply not suitable for thin-film applications because of material properties (e.g., salts, which are water soluble and which crystallize). Polymers offer mechanical and environment stability but typically have substantial absorption bands in the IR range that are associated with the chemical and structural complexity of the polymer.

Polyethylene (PE) has very low absorption across a large frequency range from the near IR up to microwave frequencies because of its simple repeating $-CH_2-$ structure. This property of PE, combined with its stability, makes it an ideal candidate for IR applications. However thin-film processing of linear-chain PE is complicated by the formation of a crystalline spherulitic structure that tends to scatter light strongly and prevents the formation of transparent films. By adding side branches to linear PE, one is able to inhibit crystallization and substantially reduce scattering. To make micrometer-thick films of PE, we first prepared a 5% branched PE (Exact Polyethylene #4033, ExxonMobil) solution in xylene at 50 °C. A film with a thickness of 1 μm was spun cast from the hot solution at 1300 rpm onto a silicon substrate. The resulting film was uniform and highly transparent, and it had a surface roughness of ~35 nm rms.

In our experiments the transmission and reflection properties of the photonic crystals were measured with a Fourier-transform IR spectrometer (Nicolet 860), a polarizer (ZnS; SpectraTech) with an angular reflectivity stage (VeeMax; SpectraTech) fitted to it, and a Nicolet IR microscope. A gold mirror was used as a background standard for the reflectance measurements.

In Fig. 1, we compare the k values (imaginary part of the refractive index associated with absorption) calculated with transmission and reflection measurements for both polystyrene and PE. The molecular structures of both polystyrene and PE are also exhibited.[10] The low absorption values of PE compared
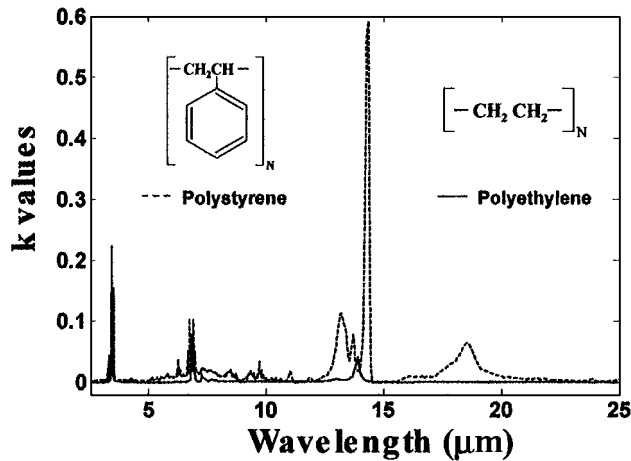
Fig. 1. Imaginary part of the refractive index (k values) describing the absorption properties of polystyrene and PE.

with those of polystyrene are a result of the simplicity of the molecular structures of PE. The spectrum of the PE exhibits absorption resonances only at 3.4 μm (2920-cm^{-1} C–H stretch mode), 6.9 μm (1450-cm^{-1} CH$_2$ scissor), and 13.9 μm (720-cm^{-1} CH$_2$ rock twist).[11]

We then used this new PE–Te material system to build an omnidirectional reflector at thermal wavelengths. Figure 2 shows a schematic of our structure, with alternating layers of Te (white regions), with refractive index n_1 and thickness h_1, and PE (gray regions), with refractive index n_2 and thickness h_2. The electromagnetic mode convention for the incoming wave with wave vector **k** is also given. Figure 3(a) shows the projected band diagram of such a structure, where the thickness ratio of the two materials is chosen to give a broadband omnidirectional reflector. In this diagram the gray areas highlight regions of propagating states, whereas the white areas represent regions containing evanescent states. The black areas represent the omnidirectional bandgap (see Ref. 7 for a detailed explanation of this band diagram). Using the film parameters $n_1 = 4.6$ (for thermally evaporated Te) and $n_2 = 1.5$ (PE), we have an omnidirectional reflecting region denoted by the black area, for a film thickness ratio of h_2 (PE)/h_1 (TE) = 1.7/0.68. The omnidirectional range has a value of 44% for our system, which we also verified by fabricating this structure and measuring the reflectivity for both polarizations at various angles (0–80°). Since a similar structure was previously investigated,[7] we do not include the results in this Letter.

The omnidirectional region for our first design exhibits a wide primary gap, but the secondary gap is very narrow [see Fig. 3(a)]. We investigated new designs to obtain two separate broad reflection regions, using only a single stack of nine layers. Obtaining a broad stop band in two different frequency regions by use of only a single stack can be of great interest for many practical purposes, for example, developing a reflective device that is functional in both solar radiation atmospheric windows.

To achieve these properties, we designed a structure by varying the thicknesses so that the secondary

bandgap would be considerably extended. This extension occurs when the PE thickness is similar to the Te thickness. Figure 3(b) shows the band diagram of a structure in which the thickness ratio was chosen as h_2 (PE)/h_1 (Te) = 1.1/0.8. The characteristic dimensionless parameter $\eta_i = 2(\omega_{h_i} - \omega_{l_i})/(\omega_{h_i} + \omega_{l_i})$ ($i = 1, 2$), which quantifies the extend of the two
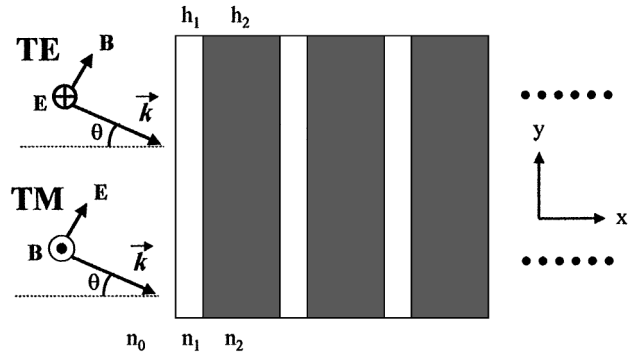

Fig. 2. Schematic of the multilayer system.
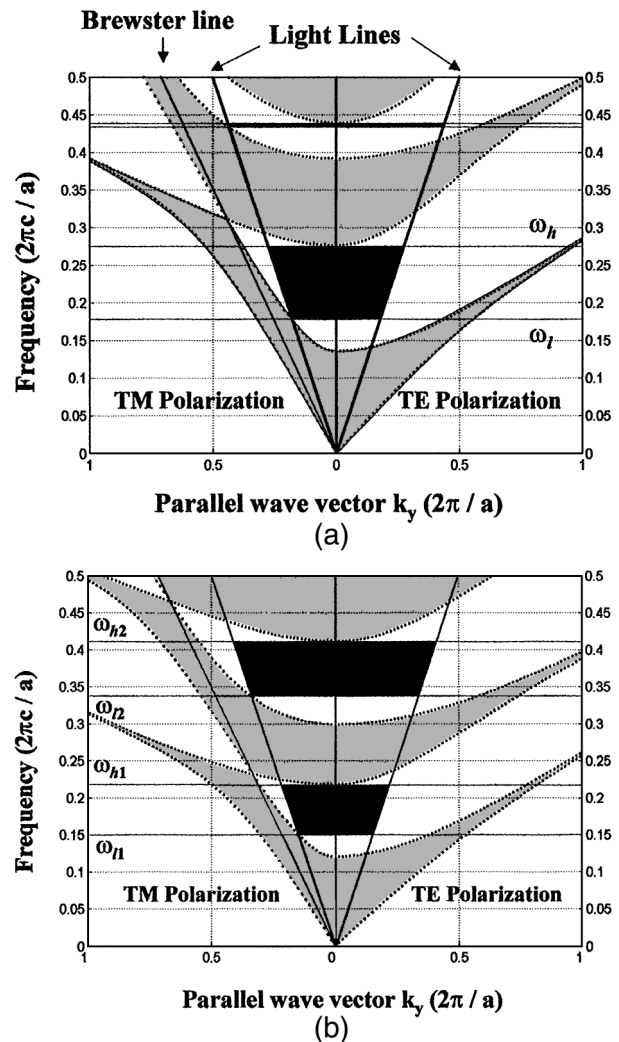

(a)

(b)

Fig. 3. Projected band structure of the multilayer film for the system of two omnidirectional reflectors, where film thickness ratio is (a) $h_2/h_1 = 1.7/0.68$, giving a single large omnidirectional band, and (b) $h_2/h_1 = 1.1/0.8$, giving two omnidirectional reflection bands.
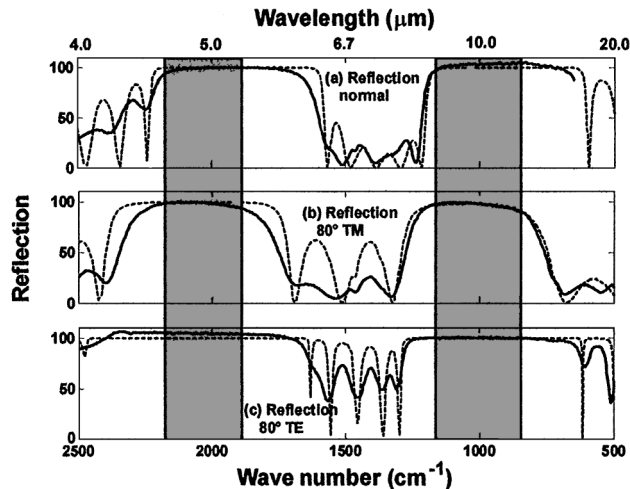
Fig. 4. Calculated (dashed curves) and measured (solid curves) reflection (in percent) for the sample that exhibits dual band at (a) normal incidence, (b) at 80° TM, and (c) at 80° TE. The gray regions show the omnidirectional reflectance frequency range.

omnidirectional ranges, has a value of 42% for the first band (lower-frequency) band and 22% for the second one (higher-frequency band).

We then fabricated this new system, using a Te layer thickness of 0.8 μm and a PE layer thickness of 1.1 μm, to match the simulated structure. Figure 4 illustrates the experimental and theoretical reflection spectra of this new nine-layer design. As can be seen from Fig. 3(b), the reflection at normal incidence (which sets the shorter-wavelength limits ω_{l1} and ω_{l2}) and the reflection of the TM-polarized wave at high angle (80° is the maximum because of experimental limitations, which sets the upper wavelength limits ω_{l1} and ω_{l2}) determine the omnidirectional reflectivity range for both bands. We demonstrate the experimental and theoretical results at normal incidence [Fig. 4(a)] and at 80° TM [Fig. 4(b)]. Reflectivity measurements at 80° for the TE-polarization [Fig. 4(c)] are included, as expected, the reflection band increases with angle for this polarization. The omnidirectional reflection ranges are highlighted in gray: the fundamental band extends from 1200 to 800 cm^{-1} (40% range/midrange ratio), whereas the higher-order band extends from 2200 to 1820 cm^{-1} (20% range/midrange ratio). The measured values of range/midrange ratio are in good agreement with the ones calculated with the band diagram. The measured reflectivity in the intermediate angles give similar high reflection values for the whole bandgap range denoted by the gray areas in Fig. 4 for both polarizations. In the simulations, we also included the

absorption, and there is very good agreement between the measured and simulated reflection spectra. The high reflectivity at all angles and both polarizations within the omnidirectional bandgap for this structure is a good verification that this new low-loss material system is proper for many applications. Moreover, the good film properties of PE yield a free-standing flexible PE−Te stack.

In conclusion, we have designed and demonstrated a low-loss all-dielectric material system that can be used to fabricate omnidirectional reflectors at a very broadband frequency range. We used the PE−Te system to investigate the formation and broadening the secondary omnidirectional bandgap. This new structure with the property of reflecting at two different regions can be used for various applications, such as in communication at atmospheric windows and waveguides with the property of omnidirectional guiding at two different wavelength regions.

References

1. E. Yablonovitch, Phys. Rev. Lett. **58,** 2059 (1987).
2. For a recent review, see articles in *Photonic Crystals and Light Localization in the 21st Century*, C. M. Soukoulis, ed., Vol. 563 of NATO ASI Series (Kluwer, Dordrecht, The Netherlands, 2001).
3. E. Ozbay, A. Abeyta, G. Tuttle, M. Tringides, R. Biswas, C. T. Chan, C. M. Soukoulis, and K. M. Ho, Phys. Rev. B **50,** 1945 (1994).
4. S. Y. Lin, J. G. Fleming, E. Chow, J. Bur, K. K. Choi, and A. Goldberg, Phys. Rev. B **62,** R2243 (2000).
5. S. Noda, Physica B **279,** 142 (2000).
6. M. Loncar, T. Doll, J. Vuckovic, and A. Scherer, J. Lightwave Technol. **18,** 1402 (2000).
7. Y. Fink, J. N. Winn, S. Fan, C. Chen, J. Michel, J. D. Joannopoulos, and E. L. Thomas, Science **282,** 1679 (1998).
8. M. Ibanescu, Y. Fink, S. Fan, E. L. Thomas, and J. D. Joannopoulos, Science **289,** 415 (2000).
9. D. N. Chigrin, A. V. Lavrinenko, D. A. Yarotsky, and S. V. Gaponenko, J. Lightwave Technol. **17,** 2018 (1999).
10. C. J. Pouchert, *The Aldrich Library of FT-IR Spectra* (Aldrich Chemical, Milwaukee, Wis., 1985), p. 1204B.
11. H. A. Szymanski, *Interpreted Infrared Spectra* (Plenum, New York, 1964), Vol. 1, pp. 19 and 35.